A Multilayered Representation, Quantum Mechanical and Molecular Mechanics Study of the CH3F+OH− Reaction in Water

ARTICLE *in* JOURNAL OF COMPUTATIONAL CHEMISTRY · MARCH 2014

Impact Factor: 3.59 · DOI: 10.1002/jcc.23498 · Source: PubMed

3 AUTHORS, INCLUDING:

Dunyou Wang
Shandong Normal University
55 PUBLICATIONS **1,744** CITATIONS

SEE PROFILE

A Multilayered Representation, Quantum Mechanical and Molecular Mechanics Study of the $CH_3F + OH^-$ Reaction in Water

Jie Chen,[a] Yulong Xu,[b] and Dunyou Wang*[a]

The bimolecular nucleophilic substitution (S_N2) reaction of $CH_3F + OH^-$ in aqueous solution was investigated using a combined quantum mechanical and molecular mechanics approach. Reactant complex, transition state, and product complex along the reaction pathway were analyzed in water. The potentials of mean force were calculated using a multilayered representation with the DFT and CCSD(T) level of theory for the reactive region. The obtained free energy activation barrier for this reaction at the CCSD(T)/MM representation is 18.3 kcal/mol which agrees well with the experimental value at ~21.6 kcal/mol. Both the solvation effect and solute polarization effect play key roles on raising the activation barrier height in aqueous solution, with the former raising the barrier height by 3.1 kcal/mol, the latter 1.5 kcal/mol. © 2013 Wiley Periodicals, Inc.

DOI: 10.1002/jcc.23498

Introduction

Bimolecular nucleophilic substitution (S_N2) reaction of the type $CH_3X + Y^- \rightarrow CH_3Y + X^-$ is a fundamental chemical reaction in organic chemistry. For the reaction of $CH_3F + OH^-$, due to the fact that F^- is a poor leaving group and this reaction is highly exothermic, it has been the subject of numerous experimental and theoretical investigations. The advent of flowing afterglow and ion-cyclotron resonance techniques in the 1970s intrigued a deep interest for this reaction in gas phase.[1–11] Until today, theoretical studies in gas phase have been the main topic for this reaction.[1–10] Even though a few experimental studies[11–14] were carried out in aqueous phase to investigate the free energy activation barrier and rate constants; however, till now, there have been no computational calculations done on the $CH_3F + OH^-$ reaction in aqueous solution.

For theoretical studies of the S_N2 reaction $CH_3F + OH^-$ in gas phase, structures, vibrational frequencies, stationary point energies, and potential energy along the intrinsic reaction coordinates and rates were calculated at all kinds of levels of theories (e.g., density function theory (DFT), Hartree-Fock method (HF), Møller-Plesset perturbation theory of the second order (MP2), coupled-cluster single double theory (CCSD), coupled-cluster single double (triple) theory [CCSD(T)]) utilizing a range of basis sets.[1–9] The *ab initio* theoretical calculations in gas phase show that the potential energy has two wells on the potential energy surface: one is in the reactant channel and the other is in the product channel.[5,6,8–10] The double well feature is expected for this S_N2 reaction in gas phase. However, these studies found the exit-channel does not have a traditional backside ion-molecule structure ($F^-\cdots CH_3OH$) in the potential energy well, instead, it forms the $CH_3OH\cdots F^-$ hydrogen-bonded complex with a hydrogen bond between the OH and F^-. Trajectory simulations by Hase group[4] show that the majority of the trajectories avoid this energy well and dissociate directly into product $CH_3OH + F^-$.

Recently, we used a hybrid multilayered representation,[15,16] quantum mechanical and molecular mechanics (QM/MM)[17,18] method to simulate the S_N2 reactions in aqueous solution.[19–22] In these approaches, by performing a multilayered DFT, CCSD(T), and electrostatic potential (ESP) theories at different stages of calculation, we shift the huge computational cost to the less expensive theories to achieve the high-accuracy free energy profile at the CCSD(T)[23] representation. These results have proved that the hybrid multilayered representation QM/MM method is a very effective and accurate way to obtain the free energy reaction pathway and accurate potential of mean force (PMF) for the S_N2 reactions in solution phase. For example, the multilayered approach under the CCSD(T)/MM representation of the $CH_3Br + OH^-$[22] reaction gives a free energy activation barrier height of 22.8 kcal/mol in aqueous solution which agrees very well with the experiment value at ~23.0 kcal/mol.[12]

As no accurate quantitative computations in aqueous solution have been done on the $CH_3F + OH^- \rightarrow CH_3OH + F^-$ reaction, so in this study, we performed the multilayered QM/MM approach to study this reaction in aqueous solution. In this study, we want to (i) find the reactant, transition state, and

[a] J. Chen, D. Wang
College of Physics and Electronics, Shandong Normal University, Jinan 250014, China
[b] Y. Xu
Department of Physics, School of Science, Qilu University of Technology, Jinan 250353
E-mail: dywang@sdnu.edu.cn

Contract grant sponsor: National Natural Science Foundation of China (D. Y. Wang), contract grant number: 11074150; Contract grant sponsor: Taishan Scholarship (D. Y. Wang)

product structures of this reaction in aqueous solution; (ii) map the minimum-energy reaction pathway and calculate the accurate PMF; (iii) determine solvation contribution and the solvent-induced polarization effect to this reaction comparing to gas phase; (iv) compare the free energy activation barrier with the experimental measurement.[12]

Methodology and System Setup

The simulations of the reaction $CH_3F + OH^- \rightarrow CH_3OH + F^-$ in water were performed using the QM/MM capabilities of NWChem computational chemistry package.[24] The details of the calculation methodology have been already discussed in prior publications.[16,25,26] The multilayered QM/MM methodology allows free energy calculations using high-accuracy coupled cluster (CC) treatment of the QM region and the MM description is applied to the solvent region. We can write the total energy of the whole system as

$$E_{\mathrm{tot}} = E^{\mathrm{int}}_{\mathrm{qm}}(\mathbf{r};\psi) + E_{\mathrm{mm}}(\mathbf{r},\mathbf{R}) + E^{\mathrm{ext}}_{\mathrm{qm}}(\mathbf{r},\mathbf{R};\rho) \quad (1)$$

where **r**, **R** are the coordinates of electrons and nuclei in QM and MM regions, and $\psi(\mathbf{r},\mathbf{R})$ is many-electron wave function of the ground state for the solute region. The first term $E^{\mathrm{int}}_{\mathrm{qm}}(\mathbf{r};\psi)$, which has the gas-phase expression, represents QM energy for the solute subsystem. The second term $E_{\mathrm{mm}}(\mathbf{r},\mathbf{R})$ describes the classical energy of the MM region. The third term, $E^{\mathrm{ext}}_{\mathrm{qm}}(\mathbf{r},\mathbf{R};\rho)$, is the interaction energy between the QM and MM subsystems, including the van der Waals, Coulomb solute–solvent nuclear interactions, and the electrostatic interactions. The electrostatic interaction energy between solute electron density $\rho(\mathbf{r}')$ and classical charges Z_I of water can be approximated as

$$\sum_{\mathrm{I}} \int \frac{Z_I \rho(\mathbf{r}')}{|\mathbf{R}_\mathrm{I} - \mathbf{r}'|} dr' = \sum_{\mathrm{i,I}} \frac{Z_I Q_i}{|\mathbf{R}_\mathrm{I} - \mathbf{r}_\mathrm{i}|} = E_{\mathrm{esp}}(\mathbf{r},\mathbf{R},Q) \quad (2)$$

where the solute electron density was replaced by the effective ESP charges Q_i such that the ESP outside the solute region is the same as that produced from the full electron density $\rho(\mathbf{r}')$.

The reaction path in solution can be characterized in terms of the PMF

$$W(\mathbf{r},\beta) = -\frac{1}{\beta} \ln \int e^{-\beta E(\mathbf{r},\mathbf{R};\psi)} \mathrm{d}\mathbf{R}, \quad \beta = \frac{1}{kT} \quad (3)$$

The free energy difference of PMF between two adjacent points, A and B, along the reaction pathway is,

$$\Delta W_{\mathrm{A,B}} = -\frac{1}{\beta} \ln \langle e^{-\beta(E_\mathrm{B} - E_\mathrm{A})} \rangle_\mathrm{A}, \quad E_\mathrm{A} = E(\mathbf{r}_\mathrm{A},\mathbf{R};\psi(\mathbf{r}_\mathrm{A},\mathbf{R})), \quad E_\mathrm{B} = E(\mathbf{r}_\mathrm{B},\mathbf{R};\psi(\mathbf{r}_\mathrm{B},\mathbf{R})) \quad (4)$$

As direct calculation of $W(\mathbf{r},\beta)$ is impractical for the CCSD(T) level of theory, we calculated free energy along the nudged elastic band (NEB) pathway using multilayered approach combining ESP, DFT, and CCSD(T) level of theory. The computation was carried out at the DFT level of theory first and then transformed to CCSD(T) level of theory to calculate the PMF. The QM region was treated with the DFT and CCSD(T) level of theory during the different stage of the PMF calculation. The free energy difference $\Delta W_{A,B}$, between two adjacent points A and B along the reaction pathway, can be computed as follows[16]:

$$\Delta W^{\mathrm{CC}}_{\mathrm{A,B}} = (\Delta W^{\mathrm{CC}\rightarrow\mathrm{DFT}}_{\mathrm{A,A}} - \Delta W^{\mathrm{CC}\rightarrow\mathrm{DFT}}_{\mathrm{B,B}}) + (\Delta W^{\mathrm{DFT}\rightarrow\mathrm{ESP}}_{\mathrm{A,A}} - \Delta W^{\mathrm{DFT}\rightarrow\mathrm{ESP}}_{\mathrm{B,B}}) + \Delta W^{\mathrm{ESP}}_{\mathrm{A,B}} \quad (5)$$

The first and second terms in brackets are the free energy difference for the representation change from the CC to DFT level of theory and from DFT to a classical ESP level of theory at the fixed solute configuration, respectively. In this work, these terms are approximated by the corresponding internal energy differences. The third term represents the free energy difference for changing solute configurations from A to B within classical ESP/MM description, and is calculated through explicit statistical sampling.

In this study, the solute OH^-/CH_3F group was treated as QM region. The reactants were embedded into a 35.1 Å cubic box consisting of 1418 water molecules which were treated as the MM region. The classical MM representation for water solution was based on simple point charge-extended (SPC/E) model[27] and the cutoff radius for classical interactions was 15 Å. QM representation was based on DFT and CCSD(T) level of theory with corresponding to DFT/MM and CCSD(T)/MM representations. DFT calculations utilized the B3LYP[28,29] exchange correlation functional and the aug-cc-pvDZ basis was used for both the DFT and CCSD(T) calculations. The initial reactant geometry was adopted from the previous gas-phase studies.[3,4] Standard Amber force field[30] van der Waals parameters were used for the quantum region.

Here were the procedures to determine the reactant, transition state, product complex for the $CH_3F + OH^-$ reaction in water and to calculate the accurate PMF along the reaction pathway.

i. The whole system was optimized and the solvent was equilibrated using dynamics simulation for 40 ps at 298 K. The initial reactant complex in water then was obtained by optimizing the full system again. For the equilibration step, the QM region was fixed and represented by the point ESP charges calculated. Following the S_N2 mechanism by breaking the C—F bond and forming the C—O bond in the reactant complex, the initial product complex was searched. The equilibration and optimization steps were also used in this step to obtain the initial product complex.
ii. The NEB[31] method was used to compute the initial reaction pathway with 10 beads from the reactant complex to product complex. After that, the geometry with the highest energy value on the NEB reaction pathway was used as the saddle point search in aqueous solution. The final transition state was confirmed to have one

imaginary frequency through the numerical frequency calculation in aqueous solution. Using the transition state geometry, the final reactant and product states were obtained by optimizing the corresponding displacements of the transition state along the negative frequency mode. Then another round of the NEB pathway was constructed again based on the final reactant, product, and transition state with 10 beads. Molecular dynamics simulations were performed on each NEB bead along the reaction pathway to equilibrate the solvent for 40 ps. Then the whole NEB reaction pathway was optimized again. This step was repeated until the NEB reaction pathway was converged.

iii. The PMF under DFT/MM and CCSD(T)/MM representations were calculated over the converged NEB reaction pathway using eq. (5).

Results and Discussions

Reactant, transition state, and product complex

The obtained final reactant complex in water is shown in Figure 1A. The anisotropic field OH^- introduced on CH_3F results in the loss of C_{3V} symmetry for $OH^-\cdots CH_3F$, which is similar to the structure in gas phase.[1–6,9] The OH^- tilted toward to one of the hydrogen atoms in the CH_3F group. In aqueous phase, the C—O and C—F bond lengths are 2.817 and 1.460 Å, both are longer than the gas-phase values 2.647 and 1.424 Å. Especially the C—O bond length 2.817 Å is much longer than 2.647 Å in gas phase[3,4] which is due to the charge screening on OH^- by the surrounding waters. In other words, the water environment reduces the interaction between the C atom and OH^-. It can be seen that the OH^- accepts five hydrogen bonds shown in Figure 1A and the bond lengths are 1.616, 1.612, 1.672, 2.034, and 2.627 Å, respectively. This solvation pattern was also observed by previous experimental[32] and theoretical studies[33] of the OH^- in aqueous phase.

The transition state geometry in water is shown in Figure 1B. It is the highest point on the free energy NEB reaction pathway. Numerical frequency calculations confirmed the presence of single imaginary frequency of 407.5*i* cm^{-1} in aqueous solution. Compared to the structure of reactant complex, the C—O bond length becomes much shorter, at the same time, the C—F bond length becomes longer. So it is in the middle of a synchronized bond-breaking and bond-formation process. In aqueous solution, the C—O and C—F bond lengths are 2.005 and 1.841 Å which are much longer than 1.976 and 1.741 Å in gas phase.[3,4] From Figure 1B, we also can see the OH^- accepts four hydrogen bonds. In addition, the structure of the transition state is characterized by the formation of a nearly planar CH_3 group.

Figure 1C shows the product complex in water, which is quite different than that in gas phase. In gas phase, there is a product complex for which F^- is attached to the OH^- group of CH_3OH.[1–6,9] With respect to the $F^- + CH_3OH$ products, the potential energy minimum for this complex has an energy of approximately −30 kcal/mol. The simulations performed by

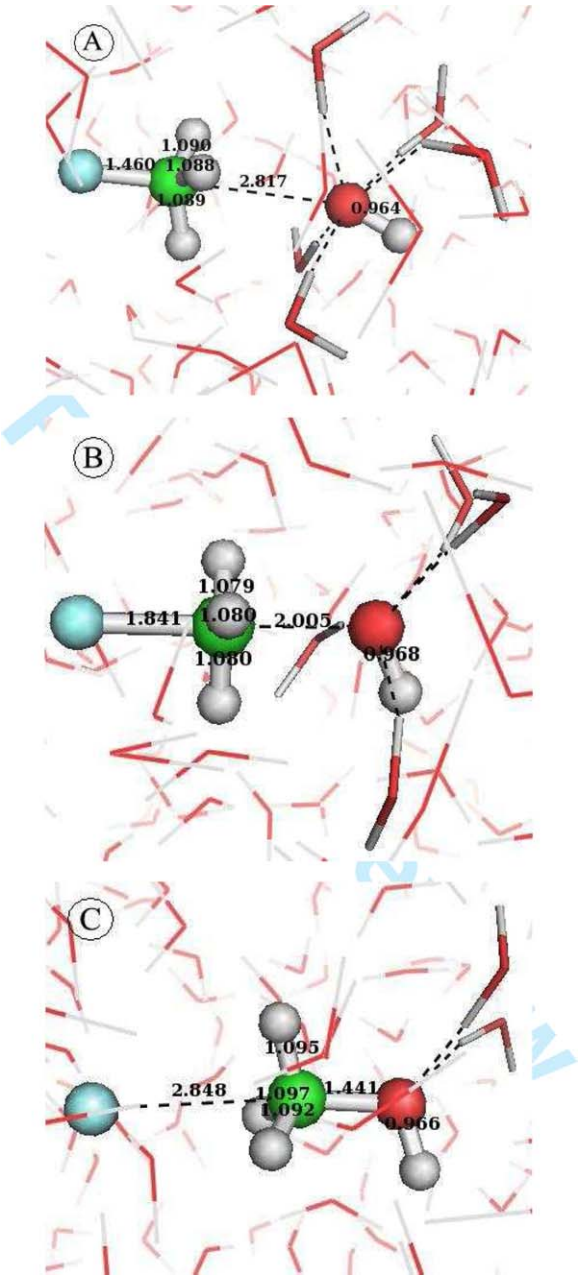

Figure 1. Structures of the A) reactant complex, B) transition state, and C) product complex for the reaction, $CH_3F + OH^- \rightarrow CH_3OH + F^-$, in aqueous solution. The units of the data in figure are angstroms. [Color figure can be viewed in the online issue, which is available at wileyonlinelibrary.com.]

Hase and coworkers[4] show that, in gas phase, only about 10% of the trajectories get trapped in this complex and most of the trajectories go directly to products. However, Figure 1C shows in the presence of water the potential energy surface on the product side of the transition state is much different from that above for the gas phase. In water, there is no longer a complex with F^- attached to the OH^- group of CH_3OH, and instead the product complex is like the traditional C_{3v} S_N2 complex with F^- attached to the backside of CH_3OH. This difference is mainly caused by the cage effect of solvent where the solvent hinders the large amplitude motions that occurs in

gas phase. The leaving F^- group was completely detached from the group CH_3 with a distance of 2.848 Å, and the new C—O bond was formed with a bond length of 1.441 Å. Thus the synchronized bond-breaking and bond-forming process was finished. We also can observe that the attacking OH^- group accepts two weak hydrogen bonds in the product complex.

Charge distribution evolution along the NEB reaction pathway

Figure 2 gives the charge evolution along the NEB reaction pathway. The first bead, the fifth, and the last bead along the NEB reaction pathway correspond to the reactant complex, transition state, and product complex for the reaction. As can be seen from the Figure 2, at the reactant state, the OH^- group has the whole negative charge at −1.0 as the substrate CH_3F keeps neutral. At the transition state, the negative charge initially concentrated on the nucleophile has been delocalized with the leaving group F and the attacking group having the same negative charge at −0.84 while the CH_3 has position charge at +0.68. At the product, the leaving group attracts the whole negative charge at −1.0 while the CH_3OH keeps neutral. It shows that the charge evolution lines of the leaving group and nucleophile are just reversed from the reactant to product with a crossing point at the transition state, which demonstrated a synchronized charge transfer process for this reaction.

Potential of mean force

The total free energy along the reaction pathway, PMF, for the reaction $CH_3F + OH^- \rightarrow CH_3OH + F^-$ under the DFT/MM, CCSD(T)/MM representations, and the solvation contribution to the total free energy are plotted in Figure 3. The PMFs were calculated in aqueous solution using eq. (5) and the solvent contribution to the free energy came from the last term in eq. (5). Only relative free energies along the reaction pathway were calculated using the reactant state as a zero reference point. This Figure shows that the DFT/MM and CCSD(T)/MM representations give almost the same PMF profiles. The free energy activation barrier for this reaction is 18.3 and 17.7 kcal/mol at CCSD(T)/MM and DFT/MM representations, respectively, which agree well with the experimental value[12] of 21.6 kcal/mol for this reaction in aqueous solution. In addition, this figure also indicates that the solvation energy contributes 3.1 kcal/mol to the transition state barrier and −18.0 kcal/mol to the reaction free energy.

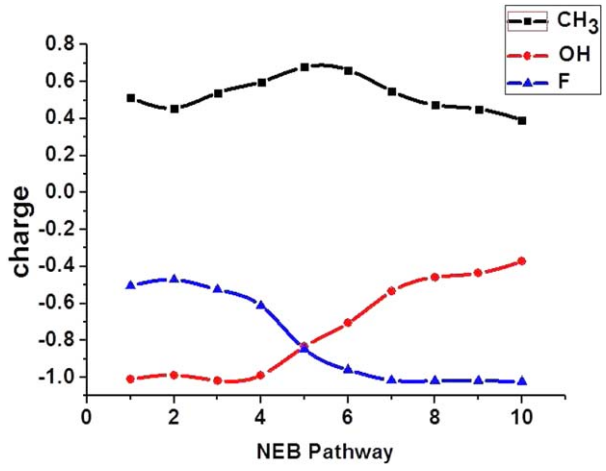

Figure 2. Charge distribution evolution of the CH_3, OH^-, and F^- along the NEB reaction pathway for the reaction $CH_3F + OH^- \rightarrow CH_3OH + F^-$. [Color figure can be viewed in the online issue, which is available at wileyonlinelibrary.com.]

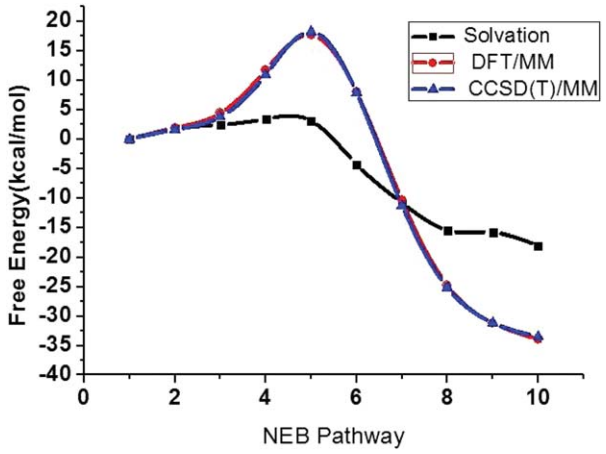

Figure 3. Free energy profiles calculated at DFT/MM, CCSD(T)/MM representations, and solvation contribution using the reactant state as a reference point.

The barrier height under the DFT level of theory is lower than the one of CCSD(T), which is consistent with previous studies that DFT systematically underestimates the reaction barrier height.[5,6,8] For this study, the DFT level of theory underestimated the barrier height by 3.9 kcal/mol comparing to the experimental value, which agrees with the theoretical benchmark study in gas phase by Truhlar group[8] that DFT/B_3LYP approach underestimates the reaction barrier heights with a mean unsigned error about 4.4 kcal/mol. Note usually the DFT calculation underestimates the barrier height on the PMF comparing with the CCSD(T) calculation. For example, the DFT barrier is 3.5 kcal/mol lower than the CCSD(T) one for $CH_3Cl + OH^-$[19] and 3.6 kcal/mol lower for the $CH_3Br + OH^-$ reaction[22] in aqueous solution. However, for the current study, the DFT barrier is only 0.6 kcal/mol lower than the CCSD(T) result. This is because that F is the most electronegative halogen atom, which forms the densest halogenated hydrocarbon. For the same type of reaction, F^- always forms the shortest distances to the center C atom comparing with other halogens throughout the reaction pathway. For example, the distances for the reactant complex, transition state, and product complex of $CH_3F + OH^-$ are much shorter at 1.460, 1.841, and 2.848 Å comparing with $CH_3Br + OH^-$ at 1.982, 2.505, and 4.026 Å[22] in water, respectively. Therefore, the DFT level of theory, which describes short-range interactions/dense matter better than long-range interactions/sparse matter, gives sufficient accurate result as the CCSD(T) level of theory for the current reaction. This phenomenon is also observed in the benchmark study of the DFT theory on the S_N2 reaction in gas

phase,[6] in which barrier heights of the DFT/B_3LYP calculation are within 1.9 kcal/mol of CCSD(T)/aug-cc-pvTZ for both the forward and reverse reaction of $CH_3OH + F^-$.

Furthermore, CCSD(T) presentation was only applied to QM solute region, and classic mechanics was used for the solution part. The discrepancy of the barrier height at CCSD(T) representation with the experimental value is mainly from the classical free energy part, which is the last term of eq. (5) describing the water solution contribution to the PMF calculated by statistical sampling. Indeed, we found the variational computational uncertainty of the sampling ranges from about $\pm$0.2 to $\pm$10.0% for the 10 configurations along the PMF reaction pathway with the maximum uncertainty at the transition state. Thus the maximum error bar on the barrier height is about $\pm$1.8 kcal/mol. Therefore, the difference of the barrier height between the CCSD(T) result and the estimated experimental value is mainly caused by the computational error of the classical energy to the PMF.

In addition, this figure also indicates that the solvation energy contributes 3.1 kcal/mol to the transition state barrier and $-$18.0 kcal/mol to the reaction free energy.

Comparison of reaction profiles

The schematic energy profiles along the reaction path in both the gas phase and solution phase for the reaction $CH_3F + OH^- \rightarrow CH_3OH + F^-$ are plotted against each other in Figure 4. The gas-phase schematic reaction pathway (green line) plotted according to both the prior experimental and theoretical studies for the $CH_3F + OH^- \rightarrow CH_3OH + F^-$ reaction in gas phase.[3,4,11] The experimental measurement in gas phase gives the heat of energy -18.0 ± 9 kcal/mol,[11] the computational benchmark value for the barrier height in gas phase is 10.89 kcal/mol[3,4] and the solvation free energies for the reactants and products are: CH_3OH[34] ($-$5.07 kcal/mol), CH_3F[34] ($-$0.22 kcal/mol), OH^-[35] ($-$106.4 kcal/mol), and F^-[36] ($-$107 kcal/mol). Combining these numbers in gas phase yields a reaction free energy of -23.45 ± 9 kcal/mol in water solution. Along with the barrier height of 21.6 kcal/mol from the experimental work,[12] the schematic estimated reaction pathway in water was also drawn in Figure 4 (blue line), which is drawn against the PMF along the reaction pathway from this study (red line). Note, the theoretical values of the solvation free energies of the reactant and product from gas phase are adopted from different theories and computations, they have different error uncertainties, thus these values' accuracy can not be justified based on one level of theory. Nonetheless, this figure shows that our PMF under the CCSD(T)/MM representation agree well with the estimated free energy reaction file in aqueous solution.

The impact of aqueous environment on this reaction comes from two aspects, one from the solvation contribution, the other from solute polarization effect. The solute polarization effect is caused by the perturbation of solute wave function by the solvent, which is shown in Figure 5 using the gas-phase energy of the reactant state as a zero reference point. Note the gas-phase reaction pathway is obtained by using the same 10 structures on the NEB reaction pathway in solution but excluding the interaction between the solute and solvent to examine the solute polarization effect. Under the DFT/MM representation, solute polarization effect raises the energy of the reactant state by 9.4 kcal/mol, transition state by 10.96 kcal/mol, and product state by 10.2 kcal/mol compared to gas phase. The net result is that solute polarization effects raises the transition state barrier height by 1.52 kcal/mol. Given the solvation contribute 3.12 kcal/mol to the barrier height, the solvation energy and the polarization effect combined to raise the activation barrier height by 4.64 kcal/mol, which means that about 1/3 of the contribution is from the polarization effect, about 2/3 from the solvation energy. This situation is

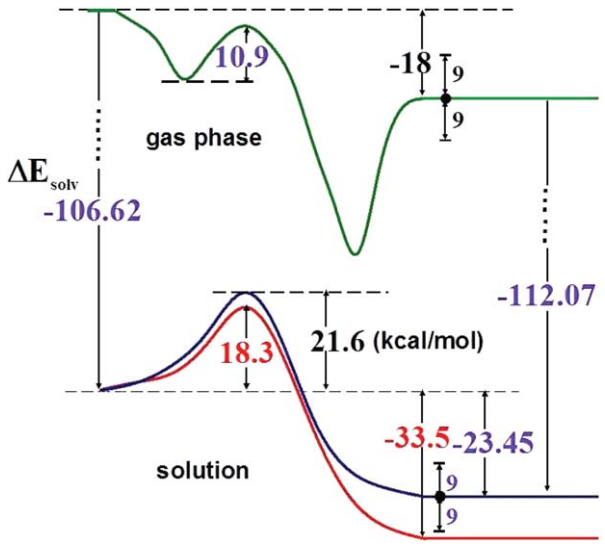

Figure 4. Comparison of free energy profiles in gas phase[3,4,11] (green curve) and in aqueous solution (red curve is the PMF from current calculation; blue is the estimated experimental one). Data labeled in black are experimental values,[11,12] and data in purple are theoretical values.[3,4,34–36]

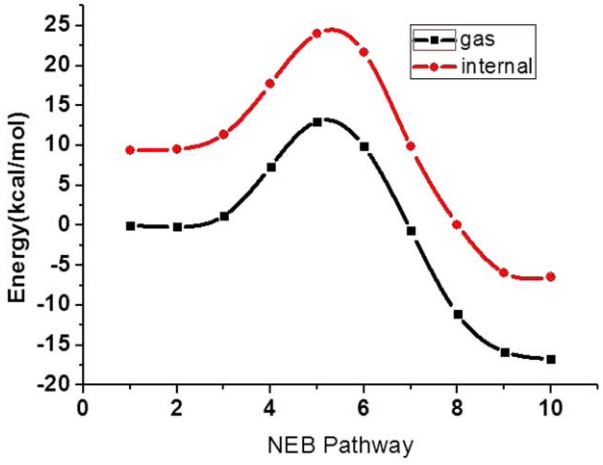

Figure 5. Comparison between gas-phase and the internal QM/MM energies along the NEB pathway at the DFT/MM representation using the gas-phase energy of the reactant as a reference point. [Color figure can be viewed in the online issue, which is available at wileyonlinelibrary.com.]

quite different than that in $CH_3Br + OH^-$ reaction,[22] in which only 8% of the contribution to the free energy barrier height is from the polarization effect, the rest is from the solvation energy. This situation is not surprising here. As F atom is more electronegative than Br, so F atom can form hydrogen bonds with the surrounding highly polar water molecules but Br atom can not, thus the solute polarization effect caused by the solvent contributes more to the barrier height than the CH_3Br case in solution.

Conclusions

As no computational studies have been done on the $CH_3F + OH^- \rightarrow CH_3OH + F^-$ reaction in aqueous solution, for the first time in this article, we performed a multilayered hybrid QM/MM study on the title reaction. The structures of reactant complex, transition state, and product complex in water were characterized. We found that the bond length of center C to the attacking group OH^- and the leaving group F in aqueous phase are commonly longer than the values in gas phase which is due to the screening effect by the surrounding water environment.

The PMF along the reaction were calculated under both the DFT/MM and CCSD(T)/MM representations. The CCSD(T)/MM theory gives an activation barrier height at 18.3 kcal/mol, which agrees well with the experimental value at 21.6 kcal/mol in solution. The DFT/MM theory shows the barrier height is at 17.7 kcal/mol, which underestimates the barrier height by 0.6 kcal/mol comparing to the CCSD(T)/MM level of theory. Nonetheless the two theories give almost the same results for this reaction.

Both the solvation energy and the solute polarization effect play important roles to shape the PMF. The solvation energy contributes 2/3 to the activation barrier height while the solute polarization effect contributes the rest. This solute polarization effect contribution is much bigger than that, 8%, in the $CH_3Br + OH^-$ case because F atom is much more electronegative than the Br atom and attracts the surrounding polar water molecules to form hydrogen bonds in aqueous solution.

Acknowledgments

The computation work was carried out at the Shanghai Supercomputer Center and Shenzhen Supercomputer Center.

Keywords: quantum mechanical/molecular mechanics • S_N2 reaction • aqueous solution • potential mean force • barrier height • reaction pathway • nucleophile

How to cite this article: J. Chen, Y. Xu, D. Wang, *J. Comput. Chem.* **2014**, *35*, 445–450. DOI: 10.1002/jcc.23498

[1] J. M. Riveros, M. Sean, G. H. Guedes, L. A. Xavier, R. F. Slepetys, *Pure Appl. Chem.* **1998**, *70*, 1969.
[2] S. El-Taher, *Int. J. Quantum Chem.* **2001**, *84*, 426.
[3] L. Sun, K. Song, W. L. Hase, M. Sena, J. M. Riveros, *Int. J. Mass Spectrom.* **2003**, *227*, 315.
[4] L. Sun, K. Song, W. L. Hase, *Science.* **2002**, *296*, 875.
[5] J. M. Gonzales, C. Pak, R. S. Cox, W. D. Allen, H. F. Schaefer, III, A. G. Csaszar, G. Tarczay, *Chem. Eur. J.* **2003**, *9*, 2173.
[6] J. M. Gonzales, R. S. Cox, III, S. T. Brown, W. D. Allen, H. F. Schaefer, III, *J. Phys. Chem. A* **2001**, *105*, 11327.
[7] A. Karton, A. Tarnopolsky, J. -F. Lamere, G. C. Schatz, J. M. L. Martin, *J. Phys. Chem. A* **2008**, *112*, 12868.
[8] Y. Zhao, N. Gonzalez-Garcia, D. G. Truhlar, *J. Phys. Chem. A* **2005**, *109*, 2012.
[9] Z. Shi, R. J. Boyd, *J. Am. Chem. Soc.* **1990**, *112*, 6789.
[10] S. Wolfe, D. J. Mitchell, *J. Am. Chem. Soc.* **1981**, *103*, 7694.
[11] K. Tanaka, G. I. Mackay, J. D. Payzant, D. K. Bohme, *Can. J. Chem.* **1976**, *54*, 1643.
[12] D. N. Glew, E. A. Moelwyn-Hughes, *Proc. R. Soc. London Ser. A. Math. Phys. Sci.* **1952**, *211*, 254.
[13] R. H. Bathgate, E. A. Moelwyn-Hughes, *J. Chem. Soc.* **1959**, *530*, 2642.
[14] I. Fells, E. A. Moelwyn-Hughes, *J. Chem. Soc.* **1959**, *72*, 398.
[15] M. Valiev, K. Kowalski, *J. Chem. Phys.* **2006**, *125*, 211101.
[16] M. Valiev, B. C. Garrett, M. -K. Tsai, K. Kowalski, S. M. Kathmann, G. K. Schenter, M. Dupuis, *J. Chem. Phys.* **2007**, *127*, 051102.
[17] J. L. Gao, D. G. Truhlar, *Annu. Rev. Phys. Chem.* **2002**, *53*, 467.
[18] A. Warshel, *Ann. Rev. Biophys. Biomol. Struct.* **2003**, *32*, 425.
[19] H. Yin, D. Wang, M. Valiev, *J. Phys. Chem. A* **2011**, *115*, 12047.
[20] D. Wang, M. Valiev, B. C. Garrrett, *J. Phys. Chem. A* **2011**, *115*, 1380.
[21] T. Wang, H. Yin, D. Wang, M. Valiev, *J. Phys. Chem. A* **2012**, *116*, 2371.
[22] Y. Xu, T. Wang, D. Wang, *J. Chem. Phys.* **2012**, *137*, 184501.
[23] R. J. Bartlett, M. Musial, *Rev. Mod. Phys.* **2007**, *79*, 291.
[24] M. Valiev, E. J. Bylaska, N. Govind, K. Kowalski, T. P. Straatsma, H. J. J. Van Dam, D. Wang, J. Nieplocha, E. Apra, T. L. Windus, W. A. de Jong, *Comput. Phys. Commun.* **2010**, *181*, 1477.
[25] M. Valiev, E. J. Bylaska, M. Dupuis, P. G. Tratnyek, *J. Phys. Chem. A* **2008**, *112*, 2713.
[26] M. Valiev, J. Yang, J. A. Adams, S. S. Taylor, *J. Phys. Chem. B* **2007**, *111*, 13455.
[27] H. J. C. Berendsen, J. R. Grigera, T. P. Straatsma, *J. Phys. Chem.* **1987**, *91*, 6269.
[28] A. D. Becke, *J. Chem. Phys.* **1993**, *98*, 5648.
[29] C. Lee, W. Yang, R. G. Parr, *Phys. Rev. B* **1988**, *37*, 785.
[30] T. Fox, P. A. Kollman, *J. Phys. Chem. B* **1998**, *102*, 8070.
[31] G. Henkelman, B. P. Uberuaga, H. Jonsson, *J. Chem. Phys.* **2000**, *113*, 9901.
[32] A. Botti, F. Brunti, S. Imberti, M. A. Ricci, A. K. Soper, *J. Mol. Liq.* **2005**, *117*, 81.
[33] M. E. Tuckerman, D. Marx, M. Parrinello, *Nature* **2002**, *417*, 925.
[34] J. Hine, P. K. Mookerjee, *J. Org. Chem.* **1975**, *40*, 292.
[35] M. W. Palascak, G. C. Shields, *J. Phys. Chem. A* **2004**, *108*, 3692.
[36] R. G. Pearson, *J. Am. Chem. Soc.* **1986**, *108*, 6109.

Received: 3 August 2013
Revised: 15 October 2013
Accepted: 10 November 2013
Published online on 25 November 2013